

## Microstructure control for developing Fe–Pd ferromagnetic shape memory alloys

To cite this article: H.Y. Yasuda *et al* 2002 *Sci. Technol. Adv. Mater.* **3** 165

View the [article online](#) for updates and enhancements.

### You may also like

- [Magnetic polyelectrolyte complex \(PEC\)-stabilized Fe/Pd bimetallic particles for removal of organic pollutants in aqueous solution](#)

Haijun Lu, Yuanshuai Li, Yuting Wang et al.

- [Avalanche criticality in thermal-driven martensitic transitions: the asymmetry of the forward and reverse transitions in shape-memory materials](#)

Antoni Planes and Eduard Vives

- [Enhancement of magnetic and surface properties in magneto-pulse electrodeposited Fe-Pd alloy thin films at various deposition potentials](#)

Soundararaj Annamalai, Arout J Chelvane and J Mohanty



# Microstructure control for developing Fe–Pd ferromagnetic shape memory alloys

H.Y. Yasuda<sup>a,b</sup>, N. Komoto<sup>a</sup>, M. Ueda<sup>a</sup>, Y. Umakoshi<sup>a,b,\*</sup>

<sup>a</sup>Department of Materials Science and Engineering, Osaka University, 2-1, Yamada-oka, Suita, Osaka 565-0871, Japan

<sup>b</sup>Frontier Research Center, Osaka University, 2-1, Yamada-oka, Suita, Osaka 565-0871, Japan

Received 14 May 2001; revised 17 November 2001; accepted 17 November 2001

## Abstract

The effect of microstructure on the ferromagnetic shape memory effect in Fe–Pd alloys was examined focusing on the orientation distribution, the grain boundary character and the grain size. Fe–29.7–31.0 at.%Pd polycrystals composed of columnar or equiaxed grains were prepared and their magnetostriction was measured under a magnetic field up to 10 kOe. The magnetostriction of the columnar crystals was much larger than that of the equiaxed ones due to the development of  $\langle 100 \rangle$  fibre texture and  $\langle 100 \rangle$  tilt grain boundary. In particular, a large magnetostriction of  $4.5 \times 10^{-4}$  was obtained even in the polycrystals. The grain boundaries of the columnar crystals also influenced the variant selection of martensites, resulting in strong dependence of the magnetostriction on the direction of magnetic field. Larger grain size did not always result in larger magnetostriction in Fe–Pd alloys. An increase in the grain size of the alloys was sometimes accompanied by the development of several sets of twin variants within a grain, resulting in a decrease in the magnetostriction. © 2002 Elsevier Science Ltd. All rights reserved.

**Keywords:** Shape memory effect; Magnetostriction; Microstructure; Orientation distribution; Grain boundary character; Grain size; Strain compatibility; Variant selection

## 1. Introduction

In the last decade, so-called multi-functional materials have been required to meet increasing demands for the performance of materials [1–3]. Shape memory alloys (SMAs) have been believed to play an indispensable role in the multi-functional materials because of their shape memory effect (SME) and superelasticity by thermoelastic martensitic transformation [4]. In general, a shape change of SMAs results from a rearrangement of martensite variants in a thermal or mechanical field. Recently, SMAs controlled by the magnetic field, so-called ‘ferromagnetic SMAs’ have recently received much attention because of their large magnetic-field-induced strain of  $10^{-2}$  order [5,6]. When ferromagnetic SMAs are subjected to an external magnetic field, the variant having favourable orientation for the field grows preferentially, resulting in a shape change [5]. In particular, a giant field-induced strain of  $6.0 \times 10^{-2}$  was

obtained in  $\text{Ni}_2\text{MnGa}$  single crystals [7]. However, from a practical viewpoint, a large magnetostriction should be obtained in polycrystalline materials, although polycrystals generally exhibit much smaller strain than the single crystals [8]. Therefore, microstructure control suitable for the ferromagnetic SME is necessary for their practical use.

Fe–Pd alloys containing 29–33 at.%Pd are known to exhibit thermoelastic martensitic transformation from fcc to tetragonal phase [9] and also to demonstrate ferromagnetic SME [10,11]. The fcc–tetragonal transformation in Fe–Pd alloys consists of expansion and shrinkage along  $a$  and  $c$  axes, respectively [9]. Thus, there are three variants depending on the selection of the  $c$  axis of tetragonal martensite among the three cubic axes of the fcc parent phase. The direction of easy magnetisation in the martensite phase is parallel to the  $a$  axis [11]. The preferential growth of specific variants whose  $a$  axis is closely parallel to the magnetic field results in a large expansion along this field. Kakeshita et al. [11] reported that Fe–31.2 at.%Pd single crystals show a maximum magnetostriction of  $3.1 \times 10^{-2}$  with magnetic field parallel to  $\langle 100 \rangle$  direction at 77 K. The obtained magnetostriction is consistent with the theoretical calculation assuming that the rearrangement of variants occurs perfectly. However, the polycrystals yielded

\* Corresponding author. Address: Department of Materials Science and Engineering, Faculty of Engineering, Osaka University, 2-1, Yamada-oka, Suita, Osaka 565-0871, Japan. Tel.: +81-6-6879-7494; fax: +81-6-6879-7495.

E-mail address: [umakoshi@mat.eng.osaka-u.ac.jp](mailto:umakoshi@mat.eng.osaka-u.ac.jp) (Y. Umakoshi).

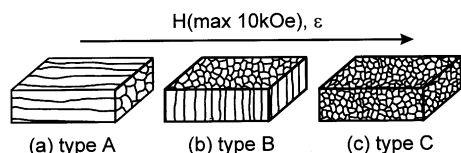


Fig. 1. Schematic illustrations of three types of Fe–Pd specimens composed of columnar (type A (a) and B (b)) or equiaxed (type C (c)) grains.

a strain of only  $1.0 \times 10^{-4}$  [12]. Furuya et al. [13] fabricated rapidly solidified Fe–Pd ribbons using an electro-magnetically controlled nozzleless melt-spinning method and obtained a magnetostriction of  $8.0 \times 10^{-4}$ . The characteristic microstructure of the rapidly solidified alloys was found to be closely related to the field-induced strain. This strongly suggests that the microstructure control in Fe–Pd polycrystals is effective in enhancing the ferromagnetic SME. In this paper, we report the effect of microstructure on the ferromagnetic SME in Fe–Pd alloys focusing on the orientation distribution, the grain boundary character and the grain size.

## 2. Experimental procedure

Master ingots of Fe–29.7–31.0 at.%Pd alloys were prepared by melting high purity Fe and Pd in a plasma arc furnace. When cooled, the columnar grains grew from a water-cooled copper hearth along the heat flow direction. After homogenising the ingots at 1373 K for 60 h, two types of Fe–Pd polycrystals were prepared: one composed of columnar grains, the other of equiaxed grains. The as-melted samples were solution-treated at 1373 K for 5 h and subsequently quenched into water, then used as columnar crystals. In contrast, the equiaxed crystals were obtained by cold rolling to 80% reduction and subsequent annealing at 1173–1573 K for 2 h. Three types of rectangular rods whose dimension is  $2 \times 2 \times 8 \text{ mm}^3$  in size were cut from the columnar and the equiaxed crystals, as schematically shown in Fig. 1. In type A and B specimens, the longitudinal direction of the columnar grains was parallel (Fig. 1(a)) and perpendicular (Fig. 1(b)) to the rods, respectively, while type C specimens were cut from the equiaxed crystals so that the rolling direction was parallel to the rods, as shown

in Fig. 1(c). The magnetostriction of these specimens, parallel to the external magnetic field up to 10 kOe was measured at various temperatures using a strain-gauge method. An optical microscope observed microstructure of these specimens. The distributions of grain orientation and grain boundary character were examined by a SEM-EBSP method.

## 3. Results and discussion

### 3.1. Microstructure of Fe–Pd alloys

Fig. 2 shows optical micrographs of type A–C specimens of Fe–29.7 at.%Pd alloys at room temperature. Type A and B specimens are composed of columnar grains with 200  $\mu\text{m}$  in average diameter and 5 mm long, as shown in Fig. 2(a) and (b), while, type C specimen recrystallised at 1573 K consists of 100  $\mu\text{m}$ -sized equiaxed grains (Fig. 2(c)). Moreover, the martensitic transformation in Fe–29.7 at.%Pd alloys occurs above room temperature. In all specimens, each grain contains a single set of twin variants of tetragonal martensites showing lamellar traces, as shown in Fig. 2(b) and (c). The lamellar traces can be seen to be almost parallel to the grain boundary traces of the columnar grains in Fig. 2(a). Furthermore, the average grain size of type C specimens depended on the recrystallisation temperature. For instance, the mean grain size increased from 6.9 to 235.0  $\mu\text{m}$  with increasing recrystallisation temperature from 1173 to 1573 K. Inverse pole figures of the fcc parent phase for the side surface of type B and C specimens of Fe–30.5 at.%Pd alloys are obtained by the SEM-EBSP method, as shown in Fig. 3. A typical  $\langle 100 \rangle$  fibre texture is well developed in the columnar crystals (Fig. 3(a)), while the orientation distribution of type C specimens is almost random (Fig. 3(b)). In particular, 83% of the columnar grains are oriented in the  $\langle 100 \rangle$  direction along the growth direction at a tolerance angle of  $20^\circ$ . The development of  $\langle 100 \rangle$  fibre texture in the columnar crystals results from the preferential growth of the cubic axis along the heat flow direction. In contrast, little recrystallisation texture is formed in type C specimens under any condition tested,

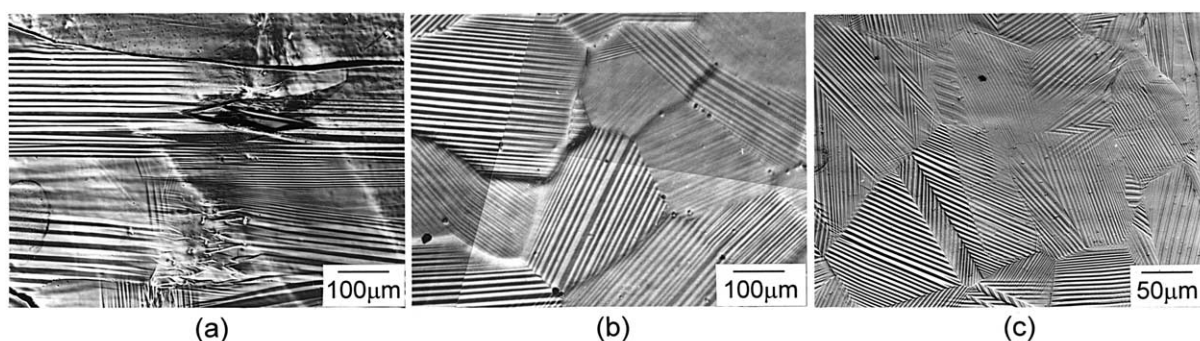


Fig. 2. Optical micrographs of Fe–29.7 at.%Pd polycrystals composed of columnar and equiaxed grains; side views of type A (a), B (b) and C (c) specimens.

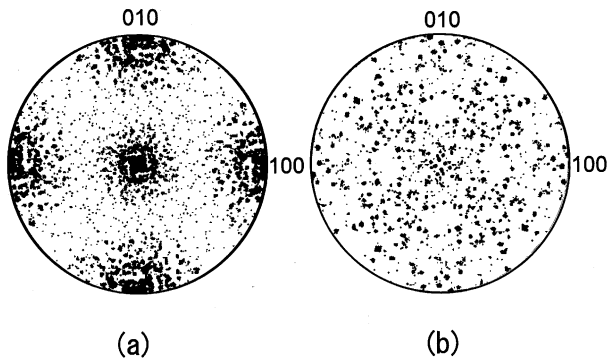


Fig. 3. Inverse pole figures of fcc parent phase for the side surface of type B (a) and C (b) specimens of Fe-30.5 at.%Pd alloy.

although the specimens were heavily cold rolled to 80% reduction.

### 3.2. Effect of orientation distribution and grain boundary character on ferromagnetic SME

Fig. 4 shows change in magnetic-field-induced strain of Fe-30.5 at.%Pd alloys at around the martensite-start temperature ( $M_s$ ) with external magnetic field. The average grain diameter of the specimens was fixed at  $150\text{ }\mu\text{m}$  to examine the effect of orientation distribution and grain boundary character on the ferromagnetic SME. The magnetostriction of Fe-Pd polycrystals depends strongly on the type of crystals. The field-induced strain of type A and B specimens composed of the columnar crystals is much larger than that of type C specimen. In the type A specimen, the magnetostriction increases rapidly with increasing magnetic field up to 2 kOe and then is saturated at about  $4.5 \times 10^{-4}$ . The induced strain of type A specimen subsequently recovers just after releasing the magnetic field with little hysteresis in the magnetostriction–magnetic field relation, while type B and C specimens exhibit large hysteresis in the relation. For instance, type B specimen shows an

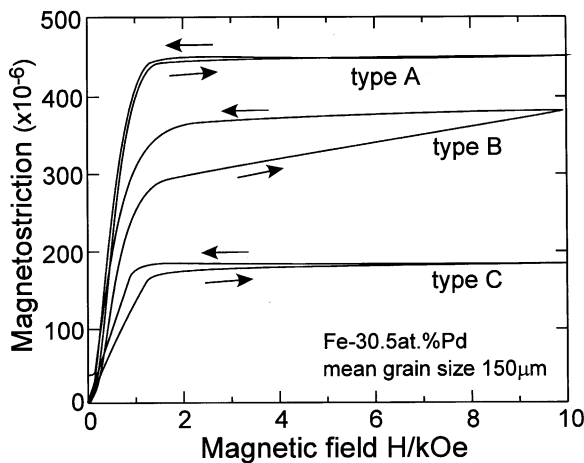


Fig. 4. Change in magnetostriction of type A, B and C specimens of Fe-30.5 at.%Pd alloys at around the  $M_s$  with magnetic field.

abrupt increase in magnetostriction with an increase in magnetic field followed by a gradual increase to  $3.5 \times 10^{-4}$ . With decreasing magnetic field, the strain obtained at 10 kOe is maintained up to 2 kOe and drops steeply to almost zero. Such irreversible behaviour observed in the strain–magnetic field curve is believed to result from the rearrangement of martensite variants by the applied magnetic field. The maximum magnetostriction of Fe-31.2 at.%Pd single crystal was reported to be  $3.1 \times 10^{-2}$  [11], much higher than that of Fe-30.5 at.%Pd polycrystals used in this study. However, the field-induced strain of type B and C specimens is not saturated even at 10 kOe, and a much larger strain is expected to be obtained at a magnetic field above 10 kOe. Thus, control of the microstructure in Fe-Pd alloys is effective in increasing the field-induced strain.

Fig. 5 shows temperature dependence of the magnetostriction at 10 kOe in Fe-30.5 at.%Pd polycrystals. The field-induced strain of type A specimen increases slightly with decreasing temperature. Just above the  $M_s$ , the magnetostriction suddenly rises probably due to a phonon softening [14,15]. The induced strain remains constant at  $4.5 \times 10^{-4}$  below the  $M_s$ . On the other hand, the magnetostriction of type B and C specimens shows a peak at around the  $M_s$ ; both an increase and a decrease in temperature from the  $M_s$  led to a decrease in the field-induced strain. Although the rearrangement of martensite variants remarkably occurs in type B and C specimens, the mobility of twin boundaries between the martensite variants is considered to be small, especially at lower temperatures. Therefore, the boundary migration of twin variants only occurs at around the  $M_s$ , resulting in a maximum strain at around that temperature.

The columnar crystals with strong  $\langle 100 \rangle$  fibre texture exhibited an excellent SME controlled by magnetic field compared with the equiaxed crystals which had random orientation. Since the direction of easy magnetisation of martensites is parallel to the  $a$  axis [11], a maximum

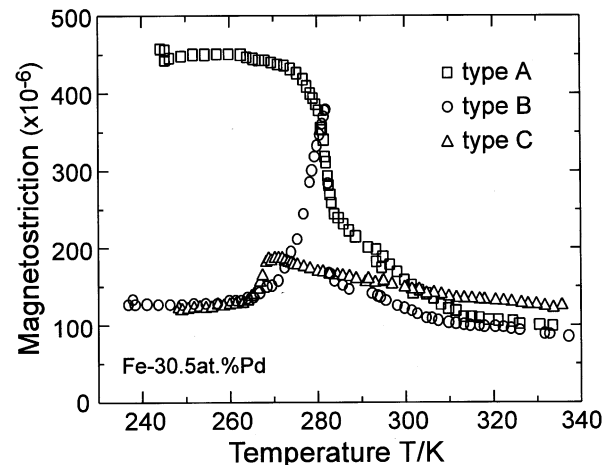


Fig. 5. Temperature dependence of magnetostriction of type A, B and C specimens at 10 kOe in Fe-30.5 at.%Pd alloy.

magnetostriction should be obtained when a magnetic field is applied parallel to  $\langle 100 \rangle$  direction. For instance, the frequencies of  $\langle 100 \rangle$  oriented grains at a tolerance angle of  $20^\circ$  in type A–C specimens of Fe–30.5 at.%Pd alloys are 83, 38 and 13%, respectively. Thus, type A and B specimens exhibit larger magnetostriction than type C.

In polycrystalline materials, a strain compatibility should be maintained at grain boundaries [16]. If the  $(x, y, z)$  cubic system whose  $y$ -axis is normal to the grain boundary is set up, the strain components in the neighbouring grains must satisfy the following equations [16]

$$\varepsilon_{xx}^1 = \varepsilon_{xx}^2, \quad \varepsilon_{zz}^1 = \varepsilon_{zz}^2, \quad \varepsilon_{xz}^1 = \varepsilon_{xz}^2 \quad (1)$$

If  $\langle 100 \rangle$  fibre texture develops perfectly in the columnar crystals, the grain boundaries can be regarded as  $\langle 100 \rangle$  tilt boundaries. The strain compatibility at  $\langle 100 \rangle$  tilt boundary is easily maintained in the columnar crystals, as described in a previous paper [17]. In general, grain boundaries constrain the shape change by applied magnetic field. However, since the compatibility requirement is readily satisfied in the columnar crystals because of the development of  $\langle 100 \rangle$  tilt boundary, suppression of the shape change by grain boundaries is thought to be small, resulting in larger magnetostriction in type A and B specimens.

The fcc to tetragonal transformation in Fe–Pd alloys consists of expansion and shrinkage along  $a$  and  $c$  axes, respectively [9]. In the martensitic transformation, there are three variants depending on the selection of  $c$  axis of tetragonal martensites among the three cubic axes of the fcc parent phase. As mentioned in our earlier paper [12], a single set of twin variants with the habit plane almost parallel to the grain boundary were preferentially selected among the six possible pairs in Fe–Pd columnar crystals. Consequently, the trace of the habit plane is almost parallel to the grain boundary traces in the columnar crystals. In that case, the  $c$  axis of selected variants is always perpendicular to the longitudinal direction of the columnar grains because of its  $\langle 100 \rangle$  fibre texture. Fig. 6 shows a schematic illustration of variant selection in type A and B specimens. In Fe–Pd alloys, the direction of easy magnetisation of tetragonal martensites is parallel to the  $a$  axis [11]. When a magnetic field is applied parallel to the columnar grains in the case of type A specimen, rearrangement of martensite variants does not necessarily occur (Fig. 6(a)), resulting in minimal hysteresis in the strain–magnetic field relation. In contrast, large hysteresis due to the reorientation of twin variants was observed in the strain–magnetic field curves of type B and C specimens. Moreover, a maximum magnetostriction in type B and C specimens was obtained at around the  $M_s$ , this also suggests that the rearrangement of twin variants occurs at around the  $M_s$  in type B and type C specimens. In contrast, the magnetostriction of type A specimens remains constant below the  $M_s$ , as shown in Fig. 6(b). Thus, the magnetostriction of type A specimen does not result from the variant reorientation, although the mechanism of shape change by applied magnetic field is not yet clear.

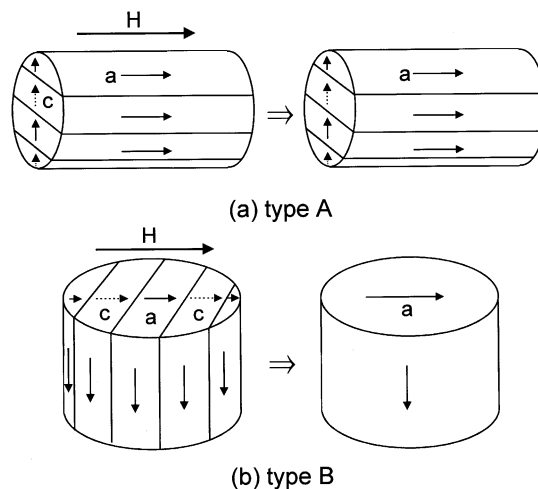


Fig. 6. Schematic illustrations showing rearrangement of variants in type A (a) and B (b) specimens in Fe–Pd alloys.

### 3.3. Grain size dependence of field-induced strain

Fig. 7 shows magnetostriction versus magnetic field curves of type C specimens of Fe–31.0 at.%Pd alloys at around the  $M_s$ . The mean grain size of type C specimens in Fe–31.0 at.%Pd alloys was controlled by changing recrystallisation temperature from 1173 to 1573 K. The field-induced strain depends strongly on the grain size. The magnetostriction increases with increasing grain size up to about  $100 \mu\text{m}$ , while further increase in grain size results in a decrease in the field-induced strain. Moreover, type C specimen with grain size less than  $50 \mu\text{m}$  shows little hysteresis in the magnetostriction–magnetic field curve. The irreversible behaviour in the strain–magnetic field relation, resulting from the reorientation of martensite variants, becomes remarkable at a grain size of  $100 \mu\text{m}$ . In contrast, the hysteresis decreases with further increase in grain size. Since the orientation distribution of type C specimens is almost random as shown in Fig. 2(b), there are many grain boundaries at which the compatibility requirement is hard to satisfy; such a grain boundary is

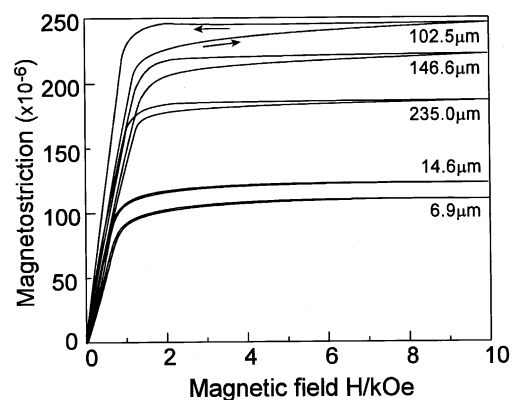


Fig. 7. Change in magnetostriction of type C specimens of Fe–31.0 at.%Pd alloys with various mean grain sizes at around the  $M_s$  with magnetic field.

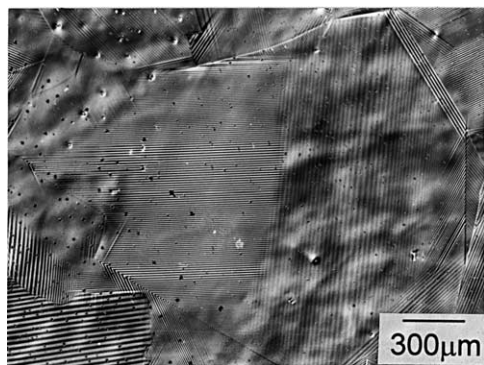


Fig. 8. An optical micrograph of Fe–31.0 at.%Pd alloys with 934  $\mu\text{m}$  in mean diameter.

believed to suppress the reorientation of twin variants. However, as the grain size increases, the constraint effect by the grain boundaries lessens resulting in a large strain due to the rearrangement of variants at larger grain size. However, further increase in grain size more than 100  $\mu\text{m}$  resulted in a decrease of magnetostriction. Fig. 8 shows an optical micrograph of Fe–31.0 at.%Pd alloys with an average grain size of 934  $\mu\text{m}$ . If the grain size becomes too large, there are many sets of variants within a grain; moreover, interpenetration of several variants is also observed. Such a complex arrangement of variants suppresses the reorientation, resulting in decrease of the magnetostriction.

#### 4. Summary and conclusions

The effect of microstructure on the field-induced strain in Fe–Pd ferromagnetic SMAs was examined, and the following conclusions were reached.

1. Fe–Pd alloys composed of columnar crystals having  $\langle 100 \rangle$  fibre texture demonstrate better ferromagnetic SME than the equiaxed grains with random orientation.
2. The compatibility requirement of transformation strain at grain boundaries is easily satisfied in the columnar crystals because of the development of  $\langle 100 \rangle$  tilt grain boundaries, resulting in enhancement of the ferromagnetic SME.
3. The variant selection of tetragonal martensites depends on grain boundaries. A limited set of twin variants with the habit plane almost parallel to the grain boundaries is preferentially chosen in the columnar crystals. Such a tendency of variant selection is closely related to the reorientation of martensite variants by applied magnetic field, especially in the columnar crystals. Moreover, the rearrangement of variants is remarkable at around the  $M_s$  in Fe–Pd polycrystals.
4. The magnetostriction of the equiaxed crystals increases with increasing grain size up to about 100  $\mu\text{m}$ , while

further increase in grain size results in a reduction in the field-induced strain.

#### Acknowledgements

This work was supported by a Grant-in-Aid for Scientific Research on Priority Area B, ‘Harmonic Material Design of Multi-Functional Composites’ from the Japanese Ministry of Education, Sports and Culture, Science and Technology. The authors would like also to thank Prof. Y. Furuya of Hirosaki University for his helpful discussion.

#### References

- [1] J.F.V. Vincent, Smart by name, smart by nature, in: G.R. Tomlinson, W.A. Bullough (Eds.), *Smart Materials and Structures*, Institute of Physics, Bristol, 1998, pp. 1–7.
- [2] A. Kumar, N.M. Ravindra, Development sensors for multifunctional applications, *JOM* 52 (2000) 14.
- [3] J. Tani, in: J. Tani (Ed.), *Smart Composites and Adaptive Structures*, Youken-do, Tokyo, 1997, pp. 1–7.
- [4] K.N. Melton, General applications of SMA's and smart materials, in: K. Otsuka, C.M. Wayman (Eds.), *Shape Memory Materials*, Cambridge University Press, Cambridge, 1999, pp. 220–239.
- [5] K. Ullakko, J.K. Huang, V.V. Kokorin, R.C. O'Handley, Magnetically controlled shape memory effect in  $\text{Ni}_2\text{MnGa}$  intermetallics, *Scripta Mater.* 36 (1997) 1133–1138.
- [6] R.D. James, K.F. Hane, Martensitic transformations and shape memory materials, *Acta Mater.* 48 (2000) 197–222.
- [7] S.J. Murray, M. Marioni, S.M. Allen, R.C. O'Handley, T.A. Lograsso, 6% magnetic-field-induced strain by twin-boundary motion in ferromagnetic Ni–Mn–Ga, *Appl. Phys. Lett.* 77 (2000) 886–888.
- [8] A. Fujita, K. Fukamichi, F. Gejima, R. Kainuma, K. Ishida, Magnetic properties and large magnetic-field-induced strains in off-stoichiometric Ni–Mn–Al Heusler alloys, *Appl. Phys. Lett.* 77 (2000) 3054–3056.
- [9] M. Sugiyama, R. Oshima, F.E. Fujita, Martensitic transformation in the Fe–Pd alloy system, *Trans. JIM* 25 (1984) 585–592.
- [10] R.D. James, M. Wuttig, Magnetostriction of martensite, *Philos. Mag.* A77 (1998) 1273–1299.
- [11] J. Koeda, Y. Nakamura, T. Fukuda, T. Kakeshita, T. Takeuchi, K. Kishio, Giant magnetostriction in Fe–Pd alloy single crystal exhibiting martensitic transformation, *Trans. Mater. Res. Soc. Jpn* 26 (2001) 215–217.
- [12] H.Y. Yasuda, N. Koumoto, Y. Umakoshi, in: T. Chandra, K. Higashi, C. Suryanarayana, C. Tome (editors), *Role of microstructure in the magnetically controlled shape memory effect in Fe–Pd alloys*, THERMEC 2000, Elsevier Science, UK 117/3 (2001) CD Rom, E7.
- [13] Y. Furuya, N.W. Hagood, H. Kimura, T. Watanabe, Shape memory effect and magnetostriction in rapidly solidified Fe–29.6at%Pd alloy, *Mater. Trans. JIM* 39 (1998) 1248–1254.
- [14] M. Masui, K. Adachi, Magnetostriction of Fe–Pd invar, *J. Magn. Mater.* 31–34 (1983) 115–116.
- [15] R. Oshima, S. Muto, F.E. Fujita, Initiation of fcc–fct thermoelastic martensitic transformation from premartensitic state of Fe–30at%Pd alloys, *Mater. Trans. JIM* 33 (1992) 197–202.
- [16] J.D. Livingstone, B. Chalmers, Multiple slip in bicrystal deformation, *Acta Metall.* 5 (1957) 322–327.
- [17] M. Ueda, H.Y. Yasuda, Y. Umakoshi, Effect of grain boundary character on the martensitic transformation in Fe–32 at.%Ni bicrystals, *Acta Mater.* 48 (2001) 3421–3432.